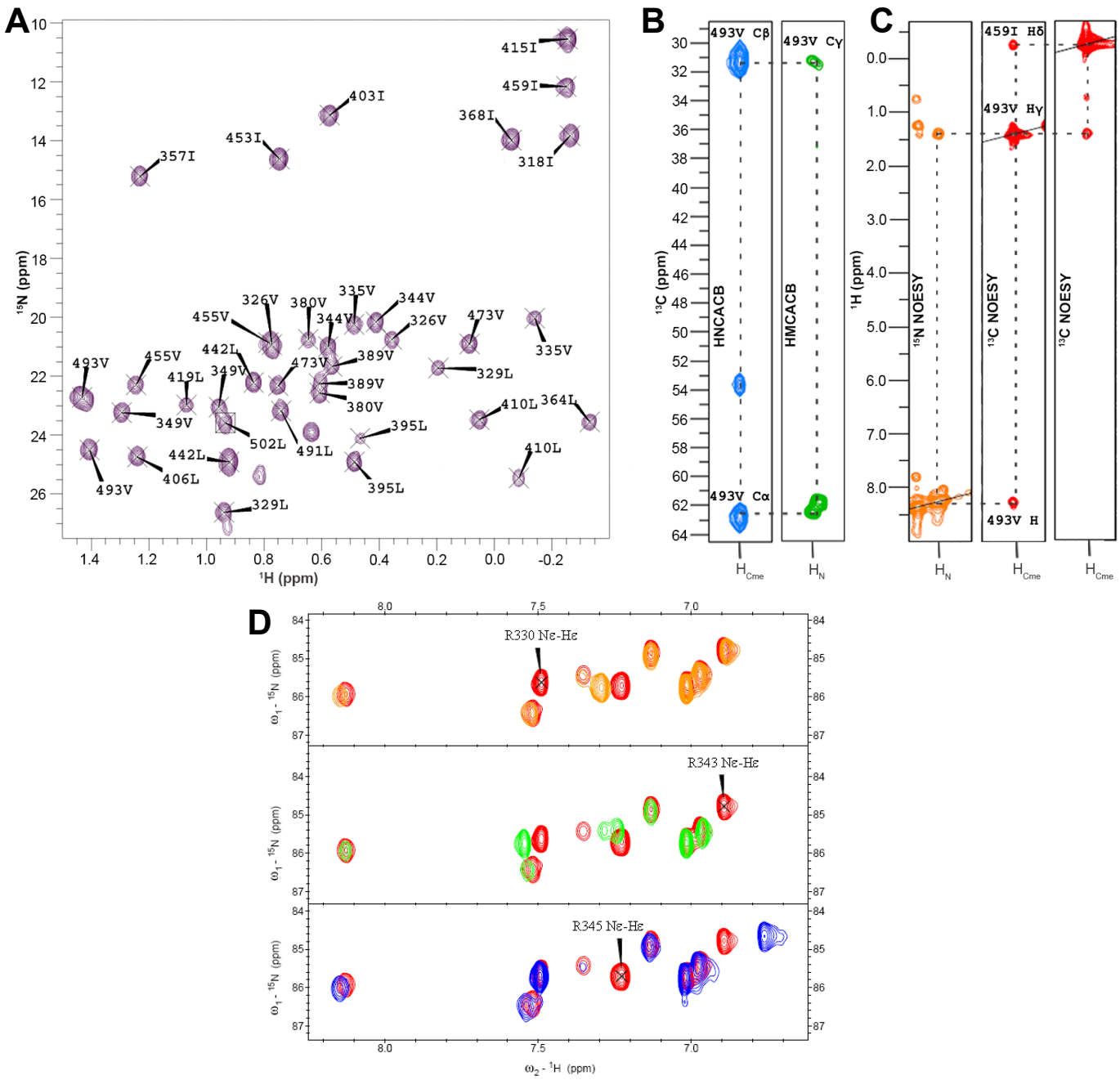

Supplemental Figure S1, Related to Figures 1 and 4. Assignment of Val/Leu/Ile methyl and Arg Nε-Hε side chain peaks.

(A) The assignments of the methyl peaks of Val, Leu, and Ile side chains in the ^{13}C HMQC spectrum are summarized.

(B) The methyl peaks were assigned by comparing through-bond correlations of the 3D HMCACB spectrum against the 3D HNCACB backbone triple resonance spectrum.

(C) NOEs aided in assignments of methyl residues with cross peaks observed to backbone amide groups and to spatially close neighboring methyl groups.

(D) The arginine side chain Nε-Hε region of the ^{15}N TROSY spectrum of wild type HPX domain (red) is superimposed with that of the R330A mutant (orange), the R343A mutant (green), or the R345A mutant (blue) in order to assign these three Nε-Hε groups at the interface with THPs. The peak assignments in Figure S1 support Figures 1B, 4.

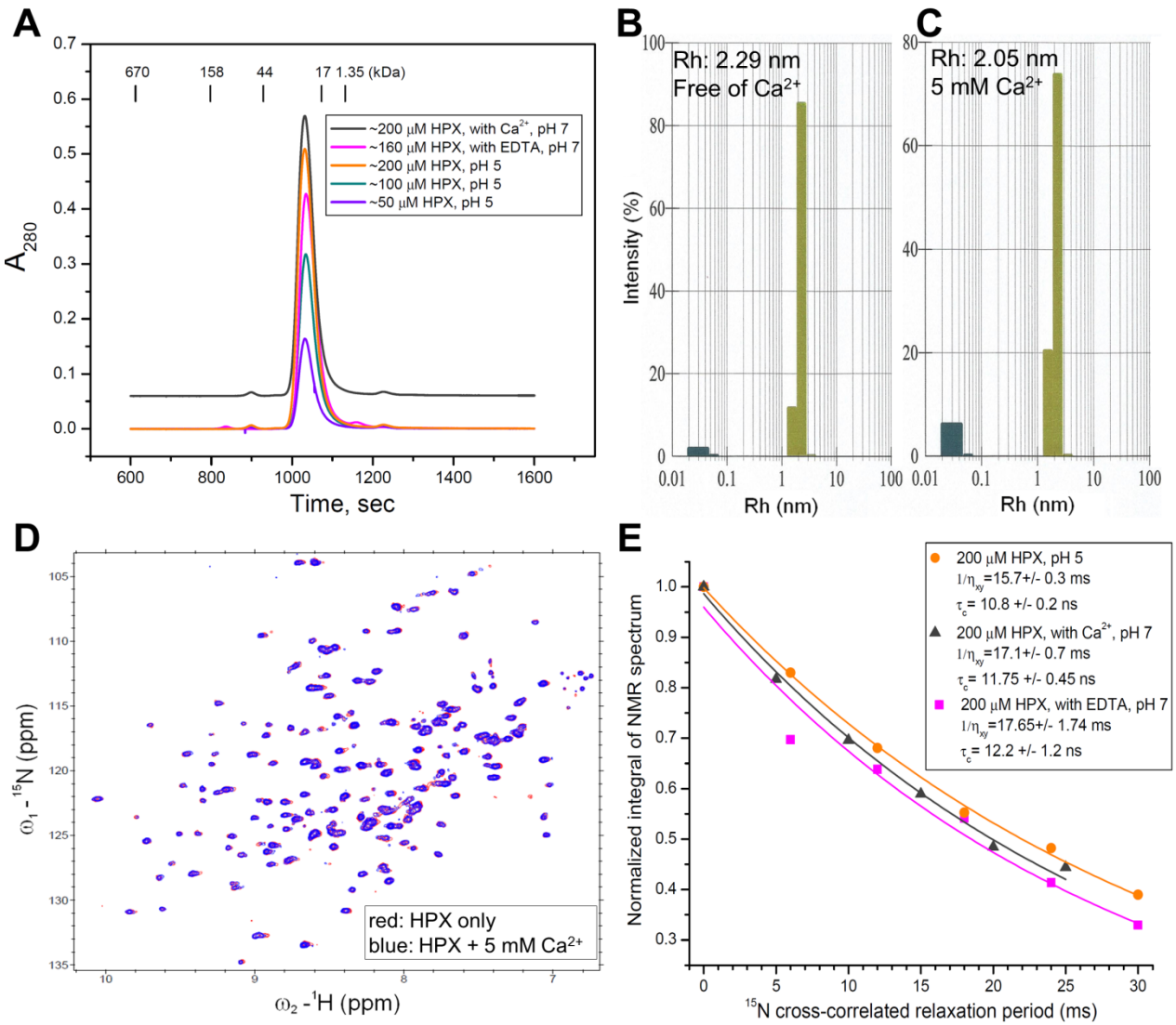

Supplemental Figure S2, Related to Figure 5A. The HPX domain of MT1-MMP is mostly monomer with minimal dependence on its concentration or on $CaCl_2$.

(A) Gel filtration was performed from 50 to 200 µM HPX domain (folded with EDTA) using a TSK G3000SW column (Tosoh) in 10 mM acetic acid (pH 5), 150 mM NaCl , or 200 µM HPX domain in 5 mM EDTA, 20 mM Tris (pH 7), 150 mM NaCl. 200 µM HPX domain folded in 5 mM Ca^{2+} was monitored by gel filtration in 5 mM $CaCl_2$, 20 mM Tris (pH 7.0), and 150 mM NaCl. Elution positions of MW standards are marked.

(B) DLS histogram of the Ca^{2+}-free peak eluting from the gel filtration column (pH 5).

(C) DLS of the peak eluting from the gel filtration column in 5 mM $CaCl_2$ at pH 7.0.

(D) ^{15}N TROSY spectra without and with 5 mM $CaCl_2$ (red and blue contours, respectively) in 20 mM Tris (pH 7.0) are superimposed, showing little difference.

(E) For estimating rotational correlation times, ^{15}N transverse cross-correlated NMR relaxation of 200 µM HPX domain (800 MHz, 37°C) was measured under conditions of (i) folding in EDTA and sample at pH 5, (ii) folding in Ca^{2+} and sample in 2.5 mM $CaCl_2$ at pH 7, and (iii) folding in Ca^{2+} and sample titrated to 5 mM EDTA at pH 7.

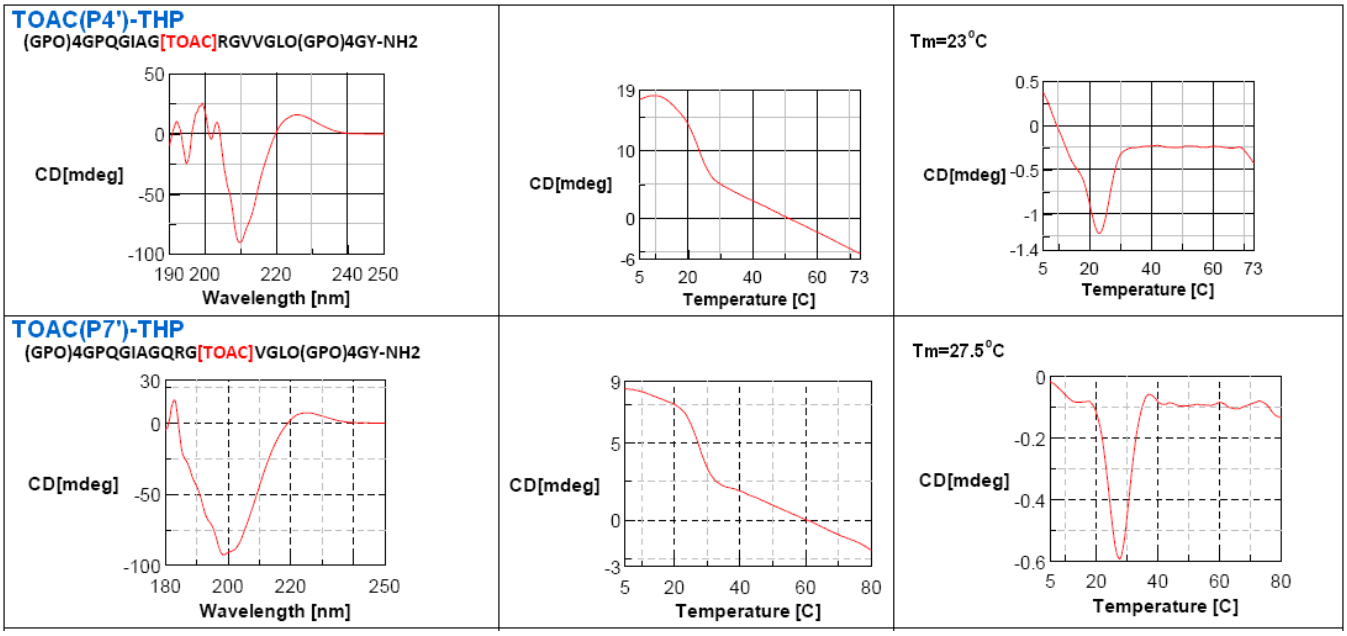

Supplemental Figure S3, Related to Figure 4. THPs with the TOAC (containing nitroxide spin label) incorporated at the P_4' or P_7' form triple helices with decreased thermal stability.

(Top panels) Characterization of α1(I)772-786 THP with TOAC substitution at the P4' position and (bottom panels) characterization of the THP with TOAC substitution at P7'. (Left panels) The positive feature in the CD spectra at λ = 225 nm indicates an intact triple-helix.

(Middle panels) The TOAC-substituted THPs were thermally melted and CD at λ = 225 nm monitored as a function of temperature.

(Right panels) First derivative plots of the melting curves indicate the melting temperature as the trough. TOAC substitutions at P_2 or P_{11}', by contrast, failed to form triple-helix and were excluded. The T_m of α1(I)772-786 THP is 41 °C.

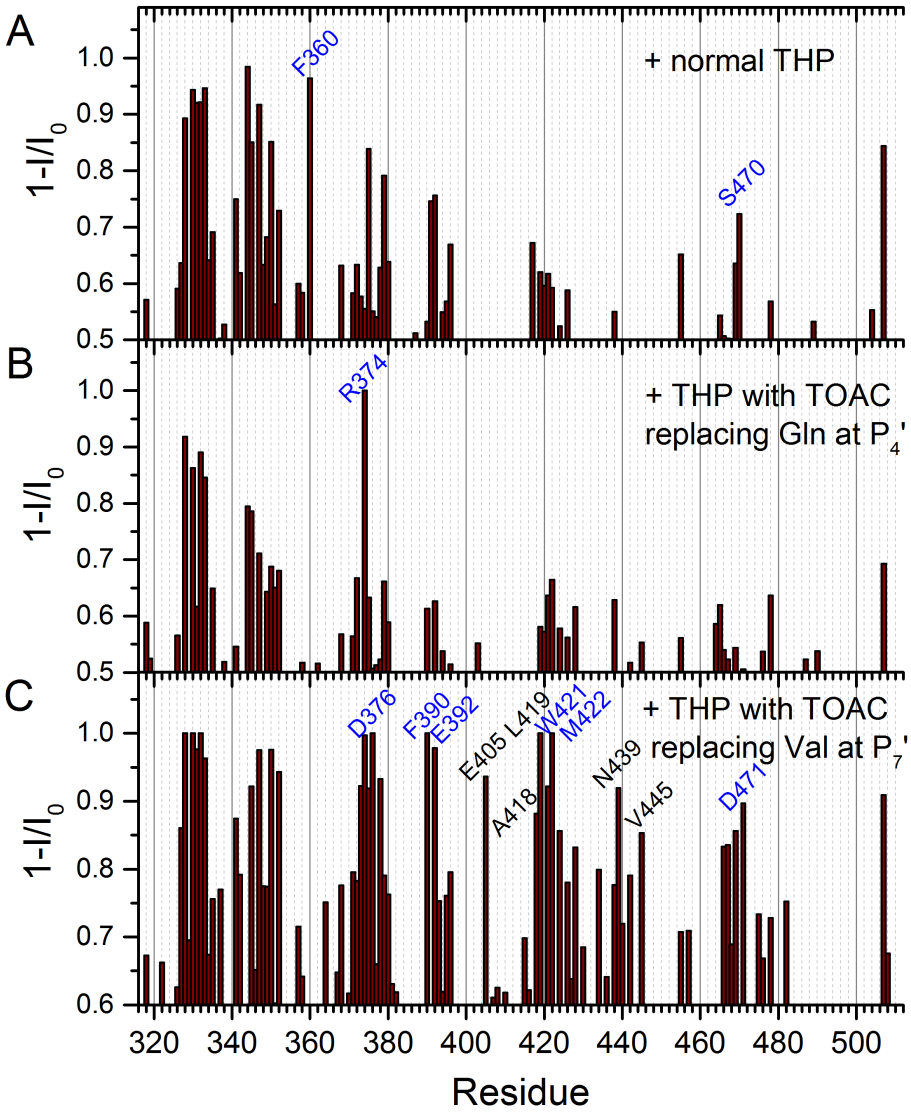

Supplemental Figure S4, Related to Figures 4 and 5. THPs without or with TOAC substitution at P_4' or P_7' induce NMR line broadening (1-I/I_0) at similar locations in the HPX domain of MT1-MMP. The conditions used were two-fold molar excess of the THP, 10 mM sodium acetate (pH 5), 0.02% NaN_3, and ^{1}H NMR frequency of 800 MHz. Labeled residues showed clearly greater NMR line broadening for that variant of the THP. Blue labeling indicates that the affected residues map to the interfacial regions suggested by Figure 1.

(A) ^{1}H-^{15}N TROSY peak heights of 300 μM HPX domain were measured at 25 °C before (I) and after (I_0) addition of two-fold excess of α1(I)772-786 THP.

(B) The peak heights of 400 μM HPX domain were measured at 12.5 °C before and after addition of two equivalents of the THP with TOAC at P_4' and 20 mM sodium ascorbate to chemically reduce the nitroxide radical and quench PREs. Figure 4A shows the site of modification.

(C) The peak heights of 400 μM HPX domain were measured at 17 °C before and after addition of two equivalents of the THP with TOAC at P_7' and 20 mM ascorbate. Figure 4B shows the site of modification. Black labels indicate residues with line broadening in blade III at greater distance from the closest approach of blade III to TOAC at P_7' (Figure 4B,D).

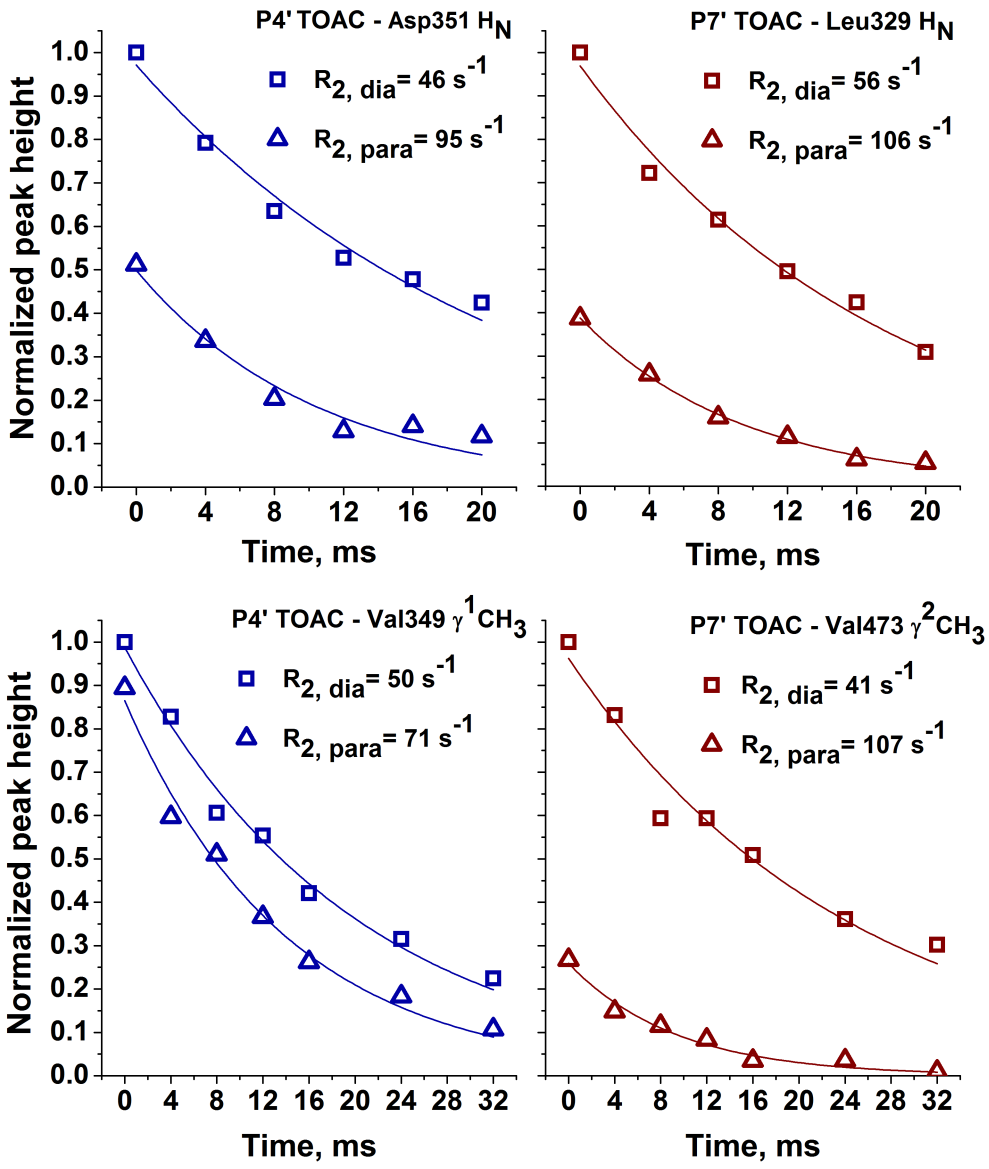

Supplemental Figure S5, Related to Figure 4. The PREs were measured as the difference between the rate constants of exponential decay of NMR peaks of the HPX domain with TOAC-labeled THP first paramagnetic and subsequently reduced to its diamagnetic state.

Exponential fits of ^{1}H R_2 relaxation were measured using CPMG trains without J coupling (Aguilar et al., 2012). Paramagnetic and diamagnetic decays revealing a PRE are illustrated for amide and methyl peaks (listed) broadened by TOAC at either the $P_{4'}$ position (blue, left panels) or $P_{7'}$ position (red, right panels) of the THP. Reduction of the unpaired electron in the TOAC nitroxide group was performed by incubation with 20 mM ascorbate for two or more hours.

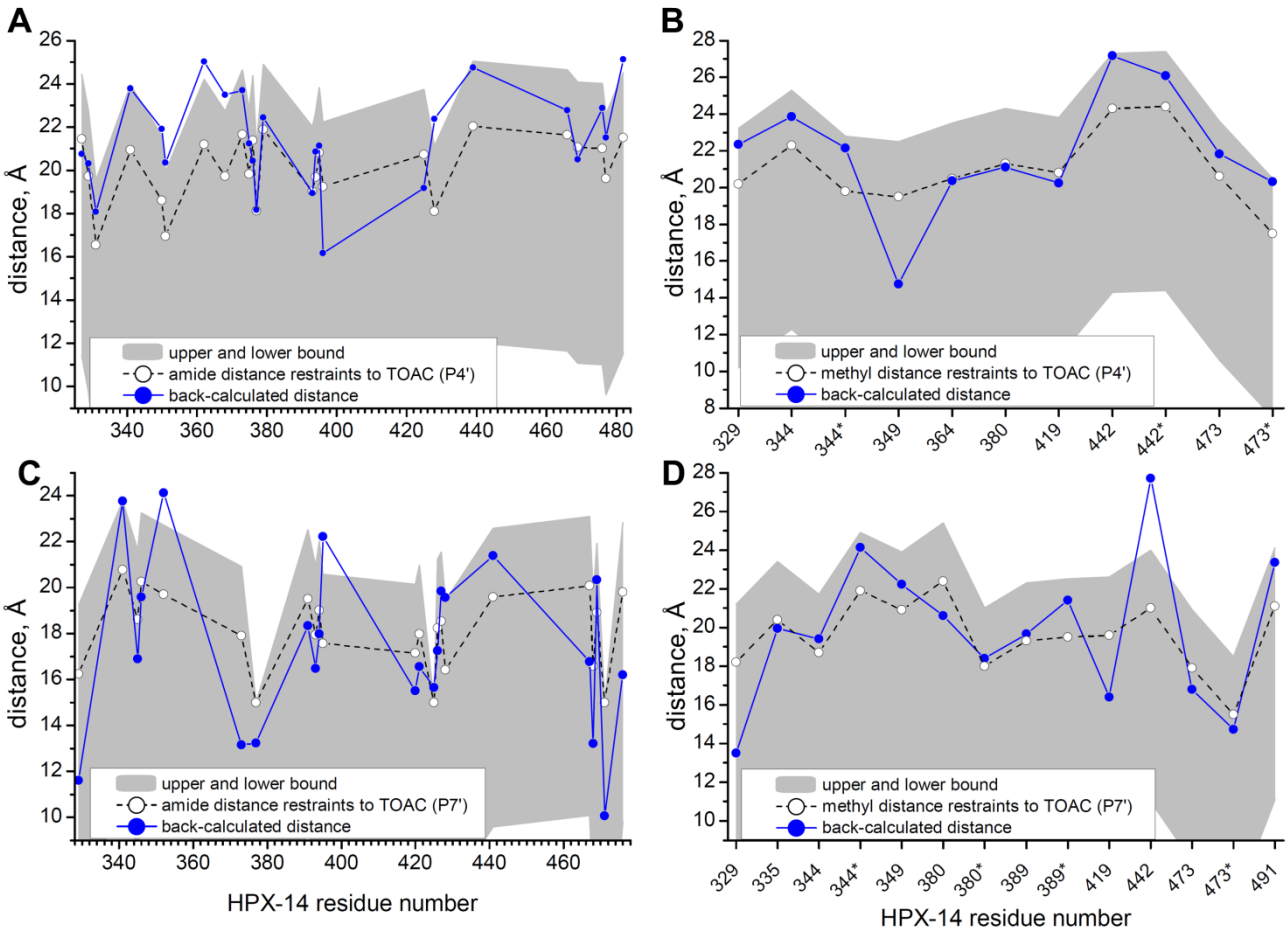

Supplemental Figure S6, Related to Figure 5. Comparison between PRE-measured distances and the corresponding distances in the best NMR structural model of the complex of THP with HPX domain from MT1-MMP (MMP-14).
(A, B) Compared are distances from TOAC at the P_4' position in the THP to amide (A) or methyl groups (B) of the HPX domain experiencing PREs.
(C, D) Compared are distances from TOAC at the P_7' position to (C) amide or (D) methyl groups of the HPX domain experiencing PREs.

Table S1, Related to Figures 5 and 7. Rotational correlation times of the HPX domain of MT1-MMP at 37 °C, measured and predicted

Quaternary structure	τ_C estimate, ns
prediction from Xtal structure	
monomer	9.1 ± 0.6 [b]
Symmetric dimer: chains A, E	23.7 ± 2.5 [b]
Measurement conditions	
Ca^{2+}-free, pH 5 [c]	10.8 ± 0.2 [d]
folded with Ca^{2+}, 5 mM Ca^{2+}, pH 7 [e]	11.75 ± 0.5 [d]
folded with Ca^{2+}, 5 mM EDTA, 2.5 mM Ca^{2+}, pH 7 [e]	12.2 ± 1.2 [d]

[a] The coordinates have PDB accession code of 3C7X (Tochowicz et al., 2011).
[b] The prediction used Fast-HYDRONMR with viscosity of 0.00692 Poise and radii of spheres at heavy atoms stepped from 2.5 to 3.7 Å as recommended (Ortega and Garcia de la Torre, 2005).
[c] Measured in 10 mM acetate buffer. EDTA was added during folding of the HPX domain to scavenge any divalent cations from the 6xHis tag.
[d] Estimated by fitting ^{15}N NMR transverse cross-correlation rate constant η_{xy} as shown in Fig. S3E and looking up the dependence of τ_C upon η_{xy} in the NMR spectral density relationship (Lee et al., 2006).
[e] Measured in 20 mM Tris buffer. 5 mM $CaCl_2$ was present during folding of the protein.

Supplemental Experimental Procedures

Expression and Isotopic Labeling of MT1-MMP Domains

The cDNA sequences encoding catalytic domain (Tyr112-Gly288), HPX domain (Pro316-Gly511), or ectodomain (Tyr112-Gly511) of human MT1-MMP were amplified by PCR with C-terminal 6xHis-tag added. The HPX and ectodomain constructs were subcloned into the pET-27b(+) expression vector and that of the catalytic domain into pET-22b(+).

$^{15}NH_4Cl$ and optionally ^{13}C-labeled glucose and D_2O were used in isotopic enrichment of the 5052 minimal medium (Studier, 2005). For selective $^{1}H/^{13}C$ protonation of Leu/Val/Ile methyl groups, 2-ketobutyric acid (50 µg/L, $^{13}C_4$-3,3-D_2-labeled, Sigma-Isotec) and α-ketovaleric acid (100 µg/L, $^{13}C_4$-3,4',4',4'-D_4-labeled, CIL) were added 1 h prior to induction with 0.5 mM IPTG. Each protein construct expressed

in *E.coli* BL21 accumulated in the inclusion bodies for 8 h until cell breakage by French press, collection, and solubilization in chaotrope: HPX or ectodomain in 5 M guanidinium HCl in 20 mM Tris·HCl (pH 7) or catalytic domain in 6 M urea in 20 mM Tris·HCl (pH 8). Each denatured domain was purified to homogeneity on nitrilotriacetic acid resin (GenScript) and eluted with 300 mM imidazole, 20 mM Tris·HCl, and the denaturant.

Folding of the HPX Domain

The HPX domain in 5 M guanidinium HCl and 20 mM Tris·HCl (pH 7) was folded by diluting to 0.05 mg/ml and dialyzing first against 3 M urea, 500 mM NaCl, 40 mM cystamine, 10 mM EDTA, and 10 mM sodium acetate (pH 5.0), next against 1 M urea and 10 mM sodium acetate (pH 5.0), and finally against 10 mM sodium acetate (pH 5.0). Samples folded in calcium replaced the last two steps with dialyses against 10 mM $CaCl_2$ and 20 mM Tris (pH 7.0), first with 1 M urea and then without it. After concentration with an Amicon centrifugal filter, NaN_3 was added to 0.02% and D_2O to 7% for NMR.

Folding of the Catalytic Domain and Ectodomain

The catalytic domain of MT1-MMP in 6 M urea was folded for enzyme kinetics by diluting to 0.1 mg/ml and dialyzing first against 3 M urea, 500 mM NaCl, 10 mM $CaCl_2$, 80 mM β-mercaptoethanol, 20 mM Tris·HCl (pH 7.5), next against 1 M urea, 10 mM $CaCl_2$, 100 μM $ZnCl_2$, 40 mM β-mercaptoethanol, 20 mM Tris·HCl (pH 7.5), and finally against 10 mM $CaCl_2$, 100 μM $ZnCl_2$, 10 mM β-mercaptoethanol, 20 mM Tris·HCl (pH 7.0).

The ectodomain and its variants in 5 M guanidinium HCl in 20 mM Tris·HCl (pH 7) were folded similarly but using the lower pH of 7.0 throughout and the final dialysis containing less β–mercaptoethanol (10 mM).

Assignment of NMR Peaks of the HPX Domain

To assign the backbone, sets of 3D HNCO, HN(CA)CO, HNCA, HN(CO)CA, HNCACB, and HN(CO)CACB spectra of the HPX domain in 10 mM acetic acid (pH 5.0) at 37 °C and independently in 20 mM Tris·HCl (pH 7.0) at 25 °C were processed with NMRPipe (Delaglio et al., 1995) and TopSpin and interpreted using Sparky.

To assign the methyl NMR peaks of Leu, Val, and Ile side chains, HMCBCA and $^{13}C/^{15}N$-edited NOESY (200 ms mixing time) spectra of a selectively methyl-protonated sample of the HPX domain in 10 mM acetic acid (pH 5.0) at 37 °C were interpreted with CCP NMR Analysis. HMCBCA skewers connect Leu/Val/Ile methyl side chains to backbone triple resonance skewers. Methyl groups were located in spatial proximity to other methyl groups using the NOEs. Stereospecific assignments of the leucine and valine methyl groups were obtained by the method of ref (Neri et al., 1989).

Hydrodynamics

The hydrodynamic radius (R_H) and polydispersity of the HPX domain were measured from dynamic light scattering using a DynaPro 99 instrument (Protein Solutions). Samples of 0.4 mM were filtered through a 0.22 μm centrifugal filter (Millipore). Twenty measurements were acquired 10 s each at a fixed angle of 90° using an incident laser beam of at 836.3 nm and analyzed using the method of cumulants.

The apparent hydrodynamic MW of the HPX domain and its concentration dependence were assayed by applying 50, 100, and 200 μM solutions to a TSK Gel G3000SW gel permeation column (Tosoh) equilibrated in 150 mM NaCl and 20 mM Tris·HCl (pH 7.5) and calibrated with MW standards.

Rotational correlation time τ_c was estimated using the using TRACT method (Lee et al., 2006) enhanced by measuring the ^{15}N NMR transverse cross-correlation rate constant η_{xy} directly using a 1D form of the pulse sequence of ref (Liu and Prestegard, 2008) on 0.2 to 0.4 mM samples ^{15}N-labeled HPX domain (pH 5). Backbone amide peaks from 8.5 to 10 ppm of well-structured regions were integrated and fitted to a single exponential decay.

Analysis of AFM Data

Images were processed using standard AFM techniques: flattening to minimize background tilt and filtering to reduce noise. A flood mask was then applied to isolate protein protrusions with an automated threshold. A smoothed second-order polynomial interpolation method was then used to decrease pixilation of the images. Peak-to-peak distances were calculated by determining local maxima within the protein, then measuring the lateral distance between the two most prominent peaks.

Structural Morphing of the MT1-MMP Ectodomain

The linker between the catalytic and HPX domain of MT1-MMP was built in Pymol in both side-by-side and sandwiching conformations. Energy minimization was further applied to the constructed linker using Sybyl. The two structures of MT1-MMPectodomain were submitted to a protein morphing server (Krebs and Gerstein, 2000) to generate the intermediate structures.

Supplemental References

Aguilar, J.A., Nilsson, M., Bodenhausen, G., and Morris, G.A. (2012). Spin echo NMR spectra without J modulation. Chem. Commun. *48*, 811-813.

Delaglio, F., Grzesiek, S., Vuister, G.W., Zhu, G., Pfeifer, J., and Bax, A. (1995). NMRPipe: a multidimensional spectral processing system based on UNIX pipes. J. Biomol. NMR *6*, 277-293.

Krebs, W.G., and Gerstein, M. (2000). The morph server: a standardized system for analyzing and visualizing macromolecular motions in a database framework. Nucleic Acids Res *28*, 1665-1675.

Lee, D., Hilty, C., Wider, G., and Wüthrich, K. (2006). Effective rotational correlation times of proteins from NMR relaxation interference. J. Magn. Reson. *178*, 72-76.

Liu, Y., and Prestegard, J.H. (2008). Direct measurement of dipole-dipole/CSA cross-correlated relaxation by a constant-time experiment. J. Magn. Reson. *193*, 23-31.

Neri, D., Szyperski, T., Otting, G., Senn, H., and Wüthrich, K. (1989). Stereospecific Nuclear Magnetic Resonance Assignments of the Methyl Groups of Valine and Leucine in the DNA-Binding Domain of the 434 Repressor by Biosynthetically Directed Fractional ^{13}C Labeling. Biochemistry *28*, 7510-7516.

Ortega, A., and Garcia de la Torre, J. (2005). Efficient, accurate calculation of rotational diffusion and NMR relaxation of globular proteins from atomic-level structures and approximate hydrodynamic calculations. J. Am. Chem. Soc. *127*, 12764-12765.

Studier, F.W. (2005). Protein production by auto-induction in high-density shaking cultures. Protein Expression Purif. *41*, 207-234.

Tochowicz, A., Goettig, P., Evans, R., Visse, R., Shitomi, Y., Palmisano, R., Ito, N., Richter, K., Maskos, K., Franke, D.*, et al.* (2011). The Dimer Interface of the Membrane Type 1 Matrix Metalloproteinase Hemopexin Domain. J. Biol. Chem. *286*, 7587-7600.